Journal Title
XX(X):1–16

Reprints and permission:
sagepub.co.uk/journalsPermissions.nav
DOI: 10.1177/ToBeAssigned
www.sagepub.com/
SAGE

Structural Fatigue and Fracture of Shape Memory Alloy Actuators: Current Status and Perspectives

Md Mehedi Hasan and Theocharis Baxevanis

Abstract

Shape Memory Alloy (SMA)-actuators are efficient, simple, and robust alternatives to conventional actuators when a small volume and/or large force and stroke are required. The analysis of their failure response is critical for their design in order to achieve optimum functionality and performance. Here, (i) the existing knowledge base on the fatigue and overload fracture response of SMAs under actuation loading is reviewed regarding the failure micromechanisms, empirical relations for actuation fatigue life prediction, experimental measurements of fracture toughness and fatigue crack growth rates, and numerical investigations of toughness properties, and (ii) future developments required to expand the acquired knowledge, enhance the current understanding, and ultimately enable commercial applications of SMA-actuators are discussed.

Keywords

Shape Memory Alloys, Actuation, Fatigue, Fracture, Phase Transformation

Introduction

Shape Memory Alloy (SMA)-based solid state actuators take advantage of the *shape memory effect* in these alloys, which stems from a reversible, solid-to-solid transformation from a low-temperature, low-order phase, termed martensite to a high-temperature, high-order phase, termed austenite upon heating (Lagoudas 2008; Otsuka and Wayman 1999). Large strains induced by the "orientation" of martensite variants can be recovered upon "reverse" phase transformation to austenite. SMA actuators offer simplicity in design, volume, dimension, and mass reduction and are, thus, an attractive alternative to conventional actuators whenever thermodynamic efficiency is not essential (Hartl and Lagoudas 2007; Sreekumar et al. 2007; Nespoli et al. 2010; Benafan et al. 2019).

Repeated thermal actuation results in gradual accumulation of dislocations due to the deformation incompatibility of the phases, which degrades the desired functionality (termed functional fatigue) of SMAs and microcracks that eventually lead to physical failure (or fracture) after sufficient number of cycles (structural fatigue) (Karakoc et al. 2017, 2019). The reversibility of phase transformation, latent heat effects, and the extreme sensitivity to chemical composition and processing-induced microstructure pose extra challenges to the effective description of the fatigue and overload fracture of SMAs as compared to that of conventional structural metals (Baxevanis and Lagoudas 2015; Karakoc et al. 2019). Given the complexity of the governing micro-mechanisms and the diversity of service conditions, predictive models and numerical methods should play a key role in understanding actuation fatigue deterioration and in design decisions for structural components.

Department of Mechanical Engineering, University of Houston, Houston, Texas

Corresponding author:
Theocharis Baxevanis, Department of Mechanical Engineering, Cullen College of Engineering, University of Houston, Houston, TX 77204-4006, US
Email: tbaxevanis@uh.edu

To facilitate the reading of the present article, it is noted that fatigue is demarcated as usual in three stages: formation, small crack growth, and long (macro) crack growth. Formation refers to nucleation and transgranular growth within the initial nucleant grain. The first two stages are concluded when the size of the fatigue crack reaches a size for which microstructural variability in the crack front is smeared out, thereby attaining similitude conditions necessary for application of fracture mechanics. The macro-cracks typically grow stably until the residual cross section is overloaded and the structure fails. Except from the stable macro-crack growth regime, the first two stages and the final overload fracture are highly sensitive to microstructure. The existing theories and methods that address fatigue are roughly categorized to (i) *total life approaches*, including all fatigue stages, *e.g.*, S–N curves, and critical plane models (Socie and Marquis 1999), and (ii) *defect tolerant approaches* that rely on fracture mechanics to estimate the crack propagation life from the largest defect (Paris and Erdogan 1963; Paris 1964). The former approaches are limited to predicting fatigue life whenever macro-crack growth occupies a small fraction of the entire life, which is the case for weight and dimension critical actuators. Both total life and defect tolerant approaches are based on empirical formulae and as such can only predict experimental results when similitude exists. Fracture is promoted ahead of the crack tip by *intrinsic* microstructural damage mechanisms, and impeded by *extrinsic* mechanisms acting primarily in the wake of the crack. Despite belonging to a relatively brittle class of materials, that of intermetallics, the intrinsic damage mechanisms in SMAs involve both cleavage of specific crystallographic planes and ductile rupture. The extrinsic shielding mechanisms, conversely, result from inelastic deformation left in the wake of the crack and nonproportional straining in the active fracture process zone. In general, crack growth in SMAs involves forward phase transformation (or orientation of self-accommodated martensite), reverse phase transformation due to elastic unloading in the wake of the crack, martensite reorientation, and nonproportional plastic deformation near the crack tip.

Mechanical (isothermal) fatigue and overload fracture in SMAs have been the subject of numerous investigations in the literature, including review papers (Plotino et al. 2009; Robertson et al. 2012; Mahtabi et al. 2015; Kang and Song 2015; Baxevanis and Lagoudas 2015) via various experimental techniques, such as synchrotron X-ray microdiffraction, IR thermography, and Digital Image Correlation (DIC) (Robertson et al. 2007; Gollerthan et al. 2009b; Zheng et al. 2017; Sgambitterra et al. 2019; Zhang et al. 2019), in contrast to actuation fatigue and fracture. Although it can be safely assumed that the micromechanisms and microstructural impact on the structural fatigue/fracture should be similar under both loading modes, temperature variations may have a profound impact on the related mechanics. Depending on the geometry, convective boundary conditions and associated heat transfer, the heating/cooling rate may result in thermal gradients and, thus, in transformation strain and stress gradients that may impact the fracture process and lifetime. Even under a uniform temperature variation resulting in forward/reverse phase transformation and thermal strains, the stress and strain fields close to a (fatigue) crack can be drastically altered. Crystallographic and martensite variants texture has been shown to affect the bulk thermal expansion (TE) response of SMAs due to the crystallographic TE anisotropy of the low-crystallographic-symmetry martensite (Monroe et al. 2016; Ahadi et al. 2017; Gehring et al. 2020). Thus, the impact of thermal strains on actuation fatigue life and the kinetics of fatigue crack growth is dependent on the mechanical loading that drives the martensite variants texture. Furthermore, the fracture criteria and fatigue indication parameters proposed for the description of the mechanical (isothermal) failure response may need to be modified to account for the thermal effects.

The focus of the present perspectives paper is to review (i) the micromechanisms of fatigue and overload fracture, assuming that they are identical irrespectively of the loading conditions, (ii) the existing experimental and theoretical/numerical work addressing structural fatigue life and fracture in SMA actuators, and (iii) discuss the experimental and modeling research priorities that may have the greatest impact on enhancing our understanding on the actuation fatigue and fracture properties of SMAs. It should be noted that the readers are assumed to be familiar with the phenomenology of the deformation response of SMAs under thermomechanical loading, which has been extensively reviewed elsewhere (Lagoudas 2008; Patoor et al. 2006; Lagoudas et al. 2006; Cisse et al. 2016).

Structural Fatigue

Micromechanisms of Fatigue

Fatigue cracks initiate on surface defects (scratches, notches, voids associated with inclusions, oxide layers formed in corrosive environment) and are associated with the formation and growth of lattice defects (Pelton 2011; Cocco et al. 2014). Formation of tongue-shaped extrusions/inclusions in polished surfaces can lead to the surface crack initiation even in the absence of any surface defects (Hornbogen and Eggeler 2004). Cracks initiate and grow on the plane of maximum shear stress and during the macro-crack propagation stage orient to the plane of maximum principal stress (Jensen 2005). The fatigue macro-crack propagation is characterized by fatigue striations and/or cleavage depending on the microstructure. Striations are finely spaced close to crack initiation site (Sawaguchi et al. 2003; McEvily and Matsunaga 2010; Chen et al. 2020) with the spacing increasing away from initiation site where large or/and shallow dimples may be formed before final failure that is indicative of fast fracture.

Experimental Investigations of Lifetime

The existing experimental investigations on actuation fatigue of SMAs are rather limited (Thumann and Hornbogen 1988; Bigeon and Morin 1996; Hornbogen 2004; Eggeler et al. 2004; Achitei et al. 2009; Bertacchini et al. 2009; Lagoudas et al. 2009; Meier et al. 2012; König et al. 2011; Dunand-Châtellet and Moumni 2012; Mammano and Dragoni 2014b; Saikrishna et al. 2013a; Karaman et al. 2013; Mammano and Dragoni 2014a; Barrera et al. 2014; Benafan et al. 2014; Karakoc et al. 2018). The available papers focus mostly to complete temperature-induced phase transformation under the constant-stress loading condition and cover a limited number of cycles (functional fatigue). The constant-stress loading condition refers to thermal variations under a constant bias load, which is an idealization of typical loading paths that utilize SMAs as actuators. In an effort to fill the gap between the test and working conditions, effects of the applied load level (Karakoc et al. 2018; Bigeon and Morin 1996; Lagoudas et al. 2009), degree of transformation (complete vs partial) (Lagoudas et al. 2009; Bhaumik et al. 2008; Bertacchini et al. 2003), loading constraints (constant stress vs constant strain) (Mammano and Dragoni 2014a), variable mechanical loading (linear stress-strain variation) (Wheeler et al. 2013; Mammano and Dragoni 2014a), upper cycle temperature (Karakoc et al. 2017, 2019), corrosion environment (Bertacchini et al. 2009; Schick 2009), and intermittent overload cycles (Saikrishna et al. 2013b) were investigated. Higher fatigue lives were observed for lower applied load levels, lower degree of transformation per cycle, constant strain as opposed to constant stress, increased slope of linear stress-strain variation, lower upper cycle temperature, and for intermittent overload cycles, respectively.

Theoretical and Numerical Investigations

Total Life Approaches The first total life approaches to actuation fatigue in SMAs involved characterizing total life to failure in terms of cyclic stress or strain range in smooth laboratory specimen under controlled conditions. These methods estimate the number of cycles to fatigue failure based on empirical formulas, such as the Basquin, $\sigma_\alpha = aN_f^b$ (Bigeon and Morin 1996; Mammano and Dragoni 2014a), and the Manson–Coffin, $\varepsilon_\alpha^p = aN_f^b$ (Lagoudas et al. 2009; Bertacchini et al. 2009), relationships, where σ_α stands for the stress amplitude, ε_α^p is the plastic strain amplitude, N_f the number of cycles to failure, and a, b are material parameters to be calibrated from experimental data. The main drawbacks of these methods for predicting actuation fatigue in SMAs is that (i) at least one of the empirical parameters a and b assumes different values for the cases of complete and partial transformation for the same constant-stress loading level, and (ii) the empirical parameters a and b can only capture a specific stress level and need to be varied for different stress conditions.

These shortcomings have been addressed by the Smith–Watson–Topper (SWT) parameter (Smith et al. 1970), which is based on the premise that fatigue life is dominated by crack initiation and growth along tensile planes, given by $\sigma_{max}\varepsilon_\alpha = aN_f^{-b}$, where ε_α is the maximum principal strain amplitude, σ_{max} is the maximum normal stress on the plane of ε_α, and a and b are material parameters (Calhoun et al. 2015). The SWT parameter belongs to the *so called* critical plane models, which relate stresses and/or strains to fatigue damage on the critical planes where fatigue cracks nucleate and grow. Thus, such models aim not only at predicting fatigue life but also the orientation of the fracture/failure plane, which are dependent on the material and loading

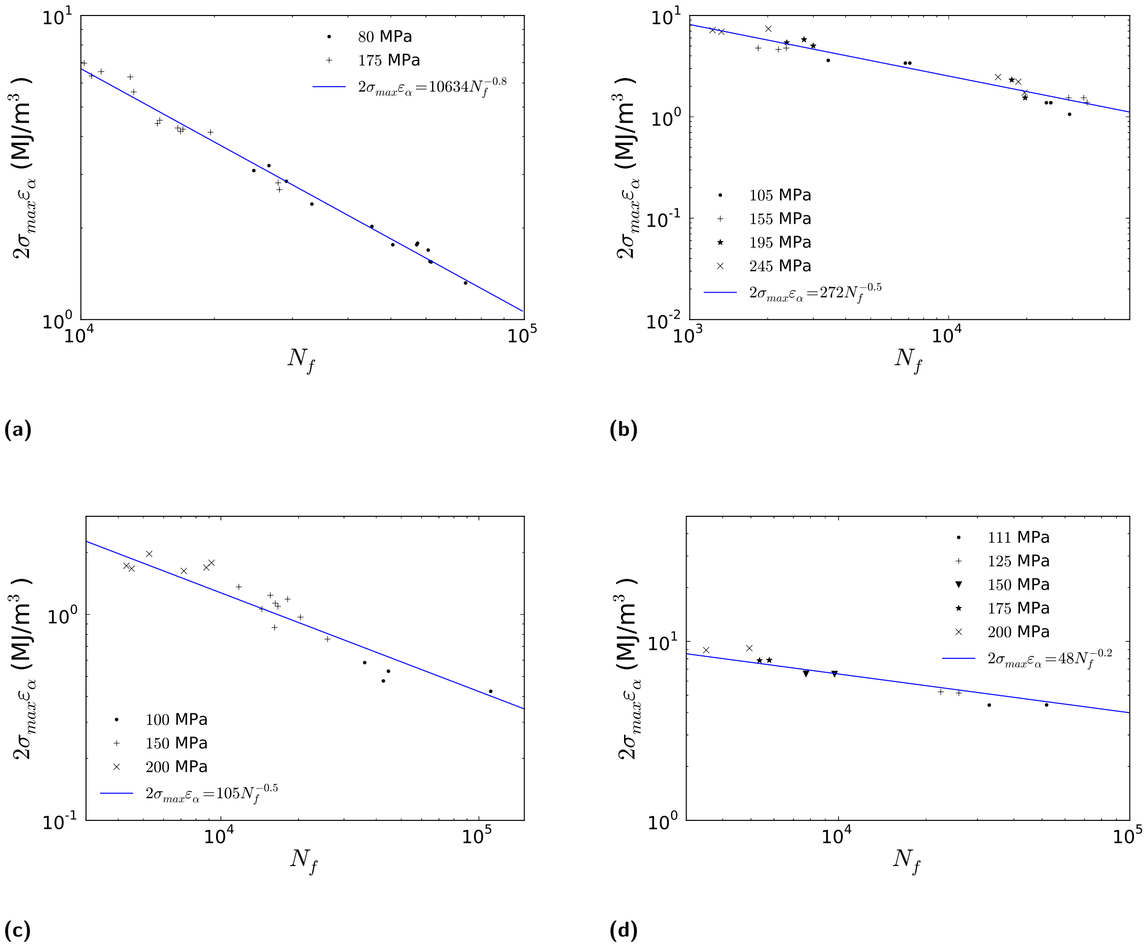

Figure 1. Relation between $\sigma_{max}\varepsilon_\alpha$ and cycles to failure N_f. (a) $Ti_{50}Ni_{40}Cu_{10}$ (Lagoudas et al. 2009). Actuation fatigue data for complete and partial transformation of various constant transformation-strain amplitudes upon cooling; (b) $Ti_{50}Ni_{40}Cu_{10}$ in a corrosive environment (Bertacchini et al. 2009). Actuation fatigue data for complete and 1% constant transformation strain amplitude upon cooling; (c) $Ni_{60}Ti_{40}$ (Schick 2009); (d) NiTi (SAES Getters SmartFlex®) (Mammano and Dragoni 2014b). After Calhoun et al. (2015).

conditions, *e.g.*, maximum shear planes or maximum tensile stress planes. As shown in Figure 1, the SWT parameter correlates well with actuation experiments under constant-stress loading. A single power law is sufficient to predict actuation lifetime of a given material system under different bias load levels and complete or partial transformation conditions.

In the aforementioned fatigue life estimates, the stress and strain fields can be safely assumed uniform for most of the specimen lifetimes and the SWT parameter can be interpreted in terms of the actuation strain energy density. For more complex configurations, *e.g.*, in the presence of notches, such as thread roots, bolt and rivet holes, which induce stress concentrations and stress gradients, fatigue life estimates are highly conservative when damage is evaluated at a critical point. Such an approach does not coincide with the fatigue damage mechanism that operates in a region of several grains (Harvey et al. 1994). The field intensity approach, which characterizes fatigue damage over a critical region, is more in line with the fatigue failure mechanisms and more comprehensive in explaining fatigue phenomena. This approach calculates an average damage evolution by integrating the damage distribution over a critical region. The field intensity approach combined with the

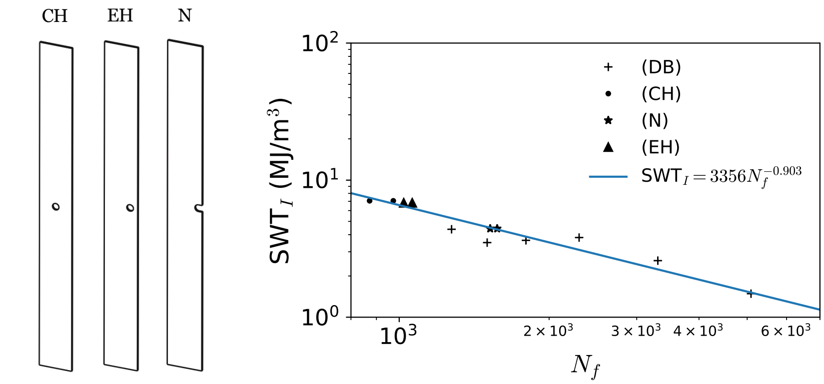

(a) **(b)**

Figure 2. (a) Plate actuator designs; (b) SWT$_I$ vs lifetime for all experiments. A least-square fit of lifetimes vs SWT$_I$ was performed over all experiments performed on the DB, CH, and N actuators to obtain the size of the domain of integration, r, and constants a and b. Note that the lifetimes of EH plates were not included in the calibration and thus the SWT$_I$ line in the figure represents a pure prediction of the experimental lifetimes for these plates. The size of the domain of integration, $r \approx 0.41$ mm is considered representative of the size of the domain in which the micro-mechanisms of fatigue damage are most active, which, in accordance to experiments, should span just a few grains. After Hasan and Baxevanis (2019).

SWT parameter takes the general form $\mathrm{SWT}_I = \frac{1}{D}\int_D \mathrm{SWT}(\mathbf{r})\varphi(\mathbf{r})dD$, where $\mathrm{SWT}(\mathbf{r}) = \sigma_{max}(\mathbf{r})\varepsilon_\alpha(\mathbf{r})$ and $\varphi(\mathbf{r})$ is a weight function that depends on the position vector $\mathbf{r}$ within a critical, highly stressed, volume domain D in which fatigue damage is expected. The weight function is introduced in order to capture configuration and size effects that originate primarily from stress gradients in a non-uniform field while in an uniform field the size effects are mainly due to variability in the number of fatigue damage sources in accordance to weakest-link statistics (Le et al. 2018). $\varphi(\mathbf{r})$ should satisfy the following properties (Weixing 1993; Yao 1996) (i) $0 \le \varphi(\mathbf{r}) \le 1$ is a decreasing function; (ii) $\varphi(\mathbf{0}) = 1$; and (iii) $\varphi(\mathbf{r}) \equiv 1$ for $\nabla\boldsymbol{\sigma} \equiv \mathbf{0}$, where $\boldsymbol{\sigma}$ is the stress tensor and the operator ∇ denotes the "gradient of". The correlation of the SWT intensity parameter with experimental data is shown for 4 different $\mathrm{Ni}_{60}\mathrm{Ti}_{40}$ (wt%) actuator geometries; dogbones (DB) and 3 plate actuator designs, *i.e.*, plates with a centered hole (CH), a notch (N), and an eccentric hole (EH) (Figure 2 and Table 1) performed by Wheeler et al. (2016). The SWT intensity parameter was evaluated from finite element calculations by employing a constitutive model for the cycling response of SMAs, the Palmgren-Miner's linear damage rule (Neuber 1960) and by assuming (i) $\varphi(\mathbf{r}) \equiv 1 - \left[1 - \frac{\mathrm{SWT}(\mathbf{r})}{\mathrm{SWT}_{\max}}\right](1+\sin\theta)r$, where r and θ are polar coordinates with respect to the notch root axis (Shang et al. 2001), and (ii) the domain of integration to be a line along the notch root axis on the surface of the specimen. The test conditions and lifetimes are given in Table 1.

Damage Tolerance Approaches The *damage tolerance* approaches to fatigue rely on fracture mechanics concepts to explicitly account for the fatigue crack growth process. These approaches typically adopt the Paris law, $da/dN = C\Delta K^m$, which relates the crack growth per cycle to the range of variation ΔK of the mode-I stress intensity factor during cyclic loading by means of the experimentally calibrated parameters C and m, and, thus, are valid only in the so-called Paris regime, *i.e.*, the stable macro-crack growth regime. *Ad hoc* modifications of the Paris power law resulted to NASGRO equation (Mettu et al. 1999), which has been shown to reproduce characteristic aspects of the fatigue response, such as crack nucleation and growth, crack closure, and maximum load effects (Rabold et al. 2013; Rabold and Kuna 2014).

The extent of phase transformation during actuation restricts the applicability of ΔK to actuation fatigue crack growth resistance in SMAs; ΔK requires the material to be deformed elastically everywhere except to a small, compared to the characteristic dimensions of the crack configuration, process zone close to the crack tip. A Paris-type power-law crack growth expression based on an extended ΔJ-integral (Lamba 1975; Tanaka 1983; Lambert et al. 1988; Banks-Sills and Volpert 1991), which accounts for thermomechanical loading, has been

Table 1. Test conditions and lifetimes. Each test was repeated twice. The uniaxial experiments show higher variability in lifetime than the rest of the specimen due to weakest-link statistics over, a larger than the high-stressed domain near the holes, gage section (Wheeler et al. 2016). The local approach, which evaluates damage at the critical point of maximum SWT parameter value, yields, as expected, highly conservative life estimates for the CH, N, and EH specimens when calibrated from the lifetimes of the DB specimens. Both the experimental and predicted lifetimes for the EH plates refer to the failure of the small ligament and not the final failure (Wheeler et al. 2016).

Geometry	Bias stress (MPa)	Test #	Cycles to failure		
			experiment	prediction	
				SWT_I	SWT
DB	200	1	5089	5194	
		2	3307	2809	
DB	250	1	2298	1828	
		2	1797	1924	
DB	300	1	1502	2007	
		2	1274	1567	
CH	118	1	973	922	238
		2	872	922	238
N	86	1	1523	1548	316
		2	1573	1548	316
EH	136	1	1062	962	152
		2	1021	962	152

recently proposed instead

$$\Delta J^* = \int_\Gamma \left[\Delta w^* dy - \Delta t_i \frac{\partial(\Delta u_i)}{\partial x} ds \right],$$

where $\Delta w^* = \int_0^{\Delta\varepsilon_{ij}} \Delta\sigma_{ij}\,(\varepsilon_{ij}, T)\, d(\Delta\varepsilon_{ij})$, $\Delta\varepsilon_{ij} = (\varepsilon_{ij})_2 - (\varepsilon_{ij})_1$, $\Delta\sigma_{ij} = (\sigma_{ij})_2 - (\sigma_{ij})_1$, $\Delta t_i = (t_i)_2 - (t_i)_1$, and $\Delta u_i = (u_i)_2 - (u_i)_1$ are variations between two loading states 1 and 2 corresponding to the beginning and end of a half cycle, σ_{ij} are the components of the stress tensor, ε_{ij} are the components of the strain tensor, u_i the components of the displacement vector, Γ is an arbitrary contour surrounding the crack tip, $t_i = \sigma_{ij} n_j$ denote the components of surface tractions, n_j the components of the unit vector normal to Γ, ds is the length increment along the contour, x and y the rectangular coordinates at the crack tip, and T is the absolute temperature. The prefix Δ designates changes in stress, strain, traction, and displacement, however, does not represent changes in J^* and w^*, which are functions of their arguments. Therefore, ΔJ^* does not correspond to the range of a J^*-integral. ΔJ^* is related to the rate of change of potential energy with respect to crack size, and scales the stress and strain fields in the crack tip deformation zone. ΔJ^* qualifies as a potential descriptor of fatigue crack growth resistance in SMAs for a wide range of thermomechanical loading paths, an assertion, which has been tested for data from both purely mechanical and actuation fatigue crack growth experiments of a high temperature shape memory alloy, $Ni_{50.3}Ti_{29.7}Hf_{20}$ (Figure 3) (Haghgouyan et al. 2021). Note that the crack growth rate data from both the isothermal mechanical and actuation loading fall approximately on the same straight line in the log–log plot. It is, thus, quite probable that the grain size (Chen et al. 2020; Lepage et al. 2018) and texture (Lepage et al. 2021) effects on the fatigue crack growth rates experimentally observed under mechanical loading to hold under actuation loading as well.

Overload Fracture

Overload fracture in SMAs usually represents the last stage of structural fatigue, once a macro-crack has grown stably until the residual cross section is overloaded and the structure fails.

Micromechanisms of Overload Fracture

Overload fracture is known to be highly sensitive to microstructure. The fracture surfaces of SMAs are characterized by both cleavage and dimples, with the latter being indicative of ductile rupture (Figure 4). Ductile rupture involves in general nucleation, growth, and coalescence of microvoids. Two clear differentiators of SMAs from other intermetallics, which may contribute to the presence of ductile rupture are their ability to transform their crystallographic structure and the presence of precipitates in large volume fractions, which act as void

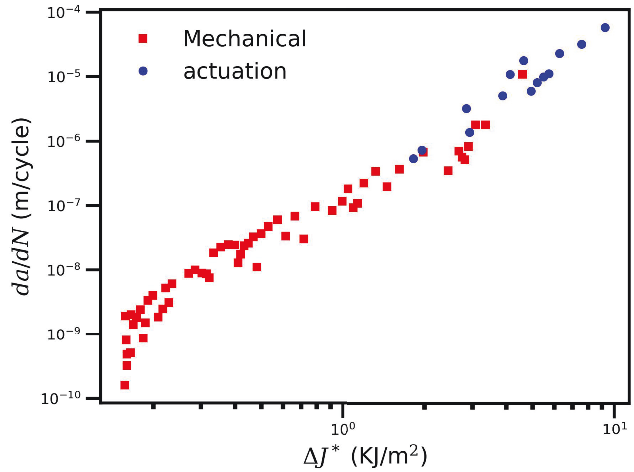

Figure 3. ΔJ^* vs da/dN plot for mechanical and actuation fatigue crack growth of NiTiHf disc compact tension specimens demonstrating a unified description of mechanical and actuation loading (Haghgouyan et al. 2021).

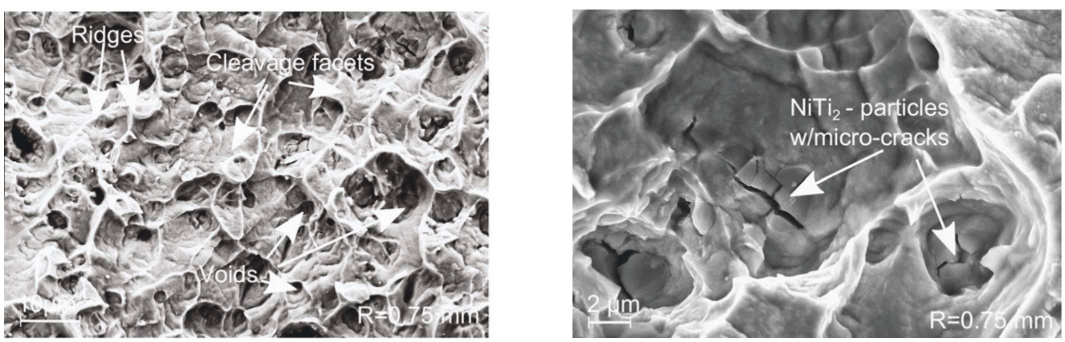

(a) **(b)**

Figure 4. SEM-images showing (a) voids, cleavage facets, and ridges, and (b) $NiTi_2$ islands with micro-cracks on the fracture surface of a specimen with $R = 0.75$mm. After Olsen et al. (2012).

initiation sites. SMAs are generally heat treated to produce metastable precipitates, of large volume fractions, which have been estimated around $2 \sim 7\%$ depending on aging (Dlouhý et al. 2004). Large second phases are also present in both Ti-rich ($NiTi_2/Ni_2Ti_4O_x$–type) and Ni-rich ($TiNi_3$-type) compositions. Decreasing Ni_4Ti_3 precipitate size in Ni-rich NiTi results in a less "ductile" response and a weaker presence of dimples in the fracture surface of SMAs (Gall et al. 1998). Similar is the effect of decreasing grain size (Ahadi and Sun 2016). The available experimental data on notched round-bars indicate that precipitation-hardened SMAs do not exhibit a softening response prior to failure. Given that void coalescence always occurs past the maximum-stress points on the effective stress–effective strain curve, it is reasonable to assume that flow localization in the intervoid ligaments is limited and that void initiation/growth is mostly followed by cleavage (Makkar and Baxevanis 2021).

Experimental Measurement of Fracture Toughness

The experimental measurement of fracture toughness is imperative in the application of fracture mechanics methods to the performance evaluation and quality assurance of SMA actuators.

The American Society for Testing and Materials (ASTM) developed fracture toughness test standards that provide guidelines on choosing and measuring the appropriate fracture parameter to characterize the fracture toughness of conventional structural metals. In brittle fracture, the energy stored in the test machine at initiation of crack advance is often higher than the energy needed to maintain crack growth and the well-defined point of the sudden load drop can be characterized by the stress intensity factor K (or the energy release rate G). Tougher materials display slow and stable crack growth, *i.e.*, the material resistance against fracture increases as the crack grows, and, thus, the fracture toughness is usually described by a resistance curve, R-curve, using the J-integral. SMAs may display both unstable (Young et al. 2019) and stable crack growth (Haghgouyan et al. 2019) depending on their composition and microstructure. Stable crack growth in SMAs is termed as transformation toughening.

A necessary modification of the ASTM standards for K and J-dominance in SMAs requires that the specimen dimensions should be large in comparison to the size of the zone of phase transformation (orientation of self-accommodated martensite) for superelastic (or martensitic) materials rather than the zone of plastic deformation; the former are usually lower than the latter. This is the only required modification for calculating fracture toughness in terms of K. For measuring fracture toughness in SMAs in terms of the J-integral, a modification of ASTM standards regarding the determination of the elastic part of the J-value, J^{el}, has been recently proposed in an effort to account for the mismatch among the apparent elastic properties of austenite, self-accommodated, and oriented martensite (Haghgouyan et al. 2019). In more recent papers (Makkar and Baxevanis 2020; Makkar et al. 2021a), (i) the expected degree of improvement in the measurement accuracy by the aforementioned proposed modification to ASTM standards, the need for further modifications regarding (ii) the uncertainty as to where to specify the fracture point on the obtained resistance curve and (iii) the specimen thickness requirement to ensure a constraint-independent measurement, as well as (iv) the dependence of the measurements on the extent of unloading in the unloading/reloading cycles used to distinguish between the elastic and inelastic components in the incremental correction of J-value for advancing cracks have been discussed. It should be noted that according to the results presented in Haghgouyan et al. (2019), the fracture toughness at temperatures below M_d corresponds to martensite and that above M_d to austenite; for nominal temperatures above M_d the austenite phase is stable and the deformation response of the SMA is similar to that of a conventional ductile metal. The fracture toughness of austenite was found considerably higher than that of martensite (Figure 5).

It should further be noted that in the literature (Gollerthan et al. 2009a; Robertson et al. 2007; Maletta et al. 2016), it was argued, based on Linear Elastic Fracture Mechanics (LEFM), that the fracture toughness of SMAs depends monotonically on temperature. However, the published data, as discussed in Baxevanis and Lagoudas (2015), appears to be determined from tests that do not comply with the small-scale transformation condition which is a perquisite for LEFM to be valid.

Recently, the first experimental measurement of the fracture toughness of SMAs under actuation loading conditions was reported (Makkar et al. 2021b). The interpretation of the data was based on an approximation of the value of the modified J^*-integral introduced in Section "Damage Tolerance Approaches" by the load–load line displacement record measured. The obtained results suggest that the employed contour integral should achieve similitude for a wide range of thermomechanical loading conditions and geometric configurations since the fracture toughness, *i.e.*, the critical $J^*_{I_C}$-values, measured under actuation loading were in close proximity to those measured under isothermal mechanical loading.

Experimental Observations of (Stable) Crack Growth under Actuation Loading

As already mentioned overload fracture usually represents the last stage of actuation fatigue, however, overload fracture may even occur due to a monotonic temperature change under a constant sufficiently high bias load. Cooling under constant applied tensile loads, which were substantially lower than the corresponding isothermal strength of the material, resulted in unstable fracture of double notched specimen NiTi (Baxevanis and Lagoudas 2015; Iliopoulos et al. 2017). Jape et al. (2021) performed experiments on pre-cracked compact tension specimens

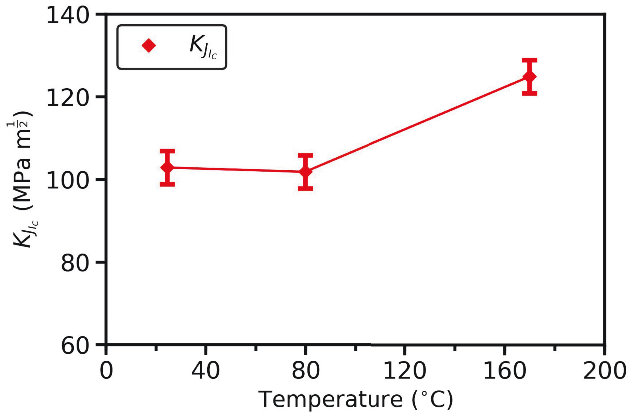

Figure 5. Extrapolated fracture toughness values, $K_{J_{I_C}}$, for NiTi CT specimens tested at $25°$C, $80°$C, and $170°$C. At $25°$C the material is in martensite state, at $80°$C the material originally in austenite phase undergoes stress-induced phase transformation, and at $170°$C the material deforms as a conventional elastic–plastic material in austenite state. The extrapolated values at temperatures $25°$C and $80°$C, which are below M_d, are found to be approximately the same (Haghgouyan et al. 2019).

under actuation loading. Such a geometry allowed for stable crack growth through multiple actuation cycles where the crack advanced during cooling for every thermal cycle and stopped once the phase transformation was completed. In all the aforementioned experiments, unstable or stable crack growth was initiated from the very first cycle and stopped in the latter cases when the driving force for crack growth, *i.e.*, phase transformation induced by cooling under a constant load, ceased, thus, these experiments can be characterized as "interrupted overload fracture" experiments. The isothermal mechanical analogue would be overload fracture under monotonic mechanical loading interrupted by unloading–reloading cycles, similar to the loading path suggested in the ASTM standards (ASTM-E561 2020; ASTM-E1820 2016) for measuring compliance and in turn crack length in constructing resistance curves.

Theoretical and Numerical Investigations

The existing numerical investigations of fracture toughness in SMAs deal almost entirely with the extrinsic shielding. These, *so called* "global", approaches do not pay attention to the failure micromechanisms. By way of contrast, the "local" approaches to fracture aim at predicting the fracture response on micromechanistical grounds.

Global Approach Thus far, only a handful of numerical investigations examined stable crack growth in SMAs under thermomechanical loading (Baxevanis et al. 2016; Jape et al. 2018, 2016). Phase transformation and transformation-induced phase transformation (TRIP) were found to affect the driving force for crack growth. Large-scale phase transformation during cooling and accumulation of TRIP over cycling in regions in front of the crack tip may (eventually) raise the driving force for crack growth above a material specific "critical" value triggering crack growth (Figure 6a), which is then stabilized by the transformation and TRIP strains left in wake of the crack (Figure 6b). Thus, transformation and TRIP strains play a dual role, raising the driving force for crack growth when in front of the crack tip and shielding the crack when left behind in the wake of the advancing crack. Depending on the bias load, either there is no crack growth or crack growth ceases once the whole material is transformed or steady-state crack growth conditions are met during cooling in the first thermal cycle (Fig. 6b)). In the former cases, multiple cooling/heating cycles are needed for crack growth to eventually reach nominally steady state conditions. Note that crack may also advance during heating as the shielding effect of transformation behind the crack tip is lost.

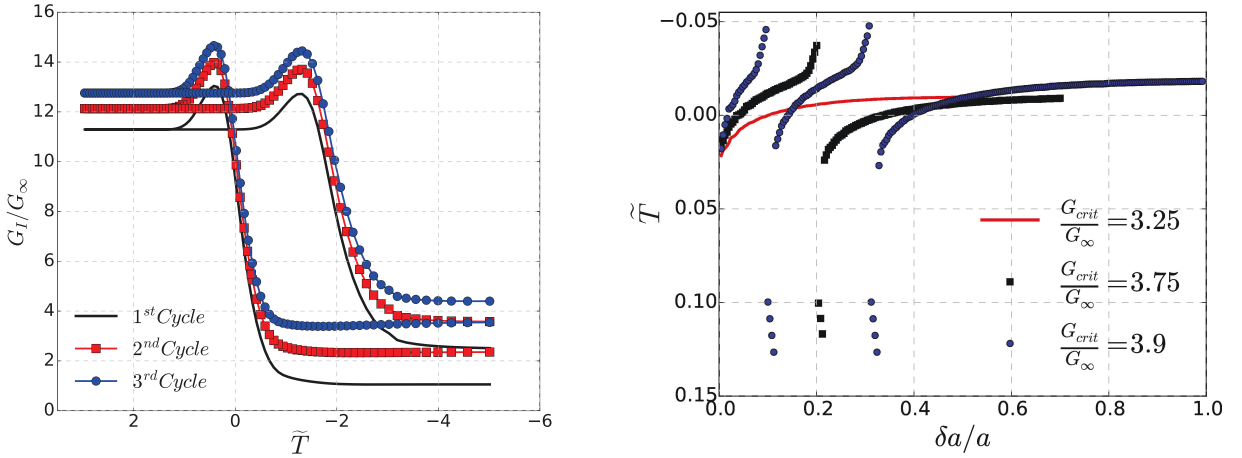

(a) **(b)**

Figure 6. (a) Evolution of the normalized crack-tip energy release rate, G_I/G_∞, versus uniform normalized temperature, $\widetilde{T}$, over three thermal cycles under a constant bias load. G_I stands for the crack tip energy release rate and G_∞ for its value due to the bias load before the first cooling. The energy release rate, *i.e.*, the driving force for crack growth, increases during cooling and can potentially result in crack advance if a material specific "critical" value is reached. The accumulation of TRIP with cycling results in higher levels of the driving force as the number of cycles increases. After Jape et al. (2018). (b) Normalized temperature, $\widetilde{T}$, vs. normalized crack growth, $\delta a/a$, showing the crack resistance "R-curve" behavior for varying bias loads. The bias load levels are normalized with respect to the critical energy release rate for initiation of crack advance, G_{cr}. The higher the ratio G_{cr}/G_∞, the smaller the bias load. Note that in Fig. 6b cooling takes place for decreasing values of the normalized temperature, $\widetilde{T}$, while in Fig. 6a is the other way around. After Jape et al. (2016).

Local Approach A constitutive model that accounts for void growth in the realm of the Gurson-Tvergaard-Needleman model, which assumes a stress-triaxiality dependence on the strain and void volume fraction evolution, has been developed in the literature but has not been applied towards the description of actuation fracture in SMAs (Bahrami et al. 2019b,a).

Perspectives

Despite the considerable progress achieved in the assessment of the mechanical fatigue and fracture response of SMAs and the transferability of part of the acquired knowledge to the respective actuation response of these materials, clearly further experimental and modeling work is needed to further enhance our understanding of the latter.

Future experimental and modeling research studies that may greatly impact the current understanding of fatigue/fracture response and practice of related mechanics concepts in SMAs are discussed below.

- *Effect of actuation loading conditions.–* Multiaxial, in- and out-of-phase, thermomechanical fatigue experiments are currently critically missing. The deformation response of SMAs under multiaxial (thermo)mechanical loading is completely different from uniaxial loading and, thus, so should the structural fatigue be as well. In service, multiaxial stress states may result from multi-directional loading, stress concentrations, or residual stresses. Similarly, there is a pressing need for torsion actuation fatigue investigations, given the recent interest in SMA toque tube actuators in the aerospace industry (Icardi and Ferrero 2009; Stroud and Hartl 2020). The available experiments on SMA toque tube actuators are limited to investigations of functional degradation under a limited number of cycles (Benafan and Gaydosh 2018; Mabe et al. 2004; Kaya et al. 2020; Akgul et al. 2020; Casati et al. 2011).
- *Small fatigue crack growth experiments.–* Compared with the behavior of corresponding large cracks at equivalent stress intensity ranges, small cracks generally display elevated growth rates and lower

fatigue threshold values (TerMaath et al. 2020; Main et al. 2021). Thus far, there have been no reported experimental tests that actually have measured small crack growth and small crack thresholds under either mechanical or actuation loading. Such measurements, which, however, are difficult to obtain and highly prone to significant scatter, are especially needed for weight critical structures, in which formation and small crack growth occupy most of the lifetime.

- *Microstructure sensitive fatigue simulations.*– Computational approaches that include the microstructure as a design variable for fatigue resistance are an emerging frontier (McDowell and Dunne 2010; Fullwood et al. 2010; Przybyla et al. 2010; Hazeli et al. 2015). Such approaches can (i) aid in the design of fatigue-resistant SMAs whereas traditional models that employ parameters fit to experimental data are not adequate for this purpose; (ii) leverage costly experimental characterization of the variability of the fatigue response; (iii) facilitate a broader exploration of the design space, reducing the development time and the associated costs; and (iv) offer promise for integration with nondestructive evaluation methods for prognosis and health monitoring.
- *Uncertainty quantification & data-driven methods.*– For physically-realistic and efficient designs, empirical safety factors should be replaced by confidence bounds that can account for the uncertainty associated with the material and mechanical properties of the component, systematic experimental noise, statistical properties of the stochastic loading, and modeling errors (Li et al. 2021; Tang et al. 2020; Sankararaman et al. 2011). Uncertainty quantification analysis may also bring into light sensitivities and correlations among physical phenomena that affect the failure response of SMAs (Honarmandi et al. 2021). Furthermore, data-driven methods offer promise as an alternative to simplistic modeling for failure prognosis, which can can only predict experimental results when similitude exists (Spear et al. 2018; Rovinelli et al. 2018; Eleftheroglou et al. 2020).
- *Local approach to fracture.*– The local approach to fracture (Lemaitre 1986; Pineau 2006) can in general assist experiments in gaining a further insight into the mechanisms that drive fracture in SMAs since the relative importance of the microstructural attributes and fracture modes, *i.e.*, void formation/growth/coalescence and cleavage, cannot be deduced from fractography, stress-strain, and R-curves alone. Such studies are expected to shed light in the role of second phase particles/grain boundaries, and the void nucleation process.

Acknowledgements

This material is based upon work supported by NASA-ULI, under Grant No. NNX17AJ96A and National Science Foundation under Grant no. CMMI-1917441.

References

Achitei D, Galuşca D, Vizureanu P, Carabet R and Cimpoeşu N (2009) Aspects regarding thermo-mechanical fatigue of shape memory alloys. *Metalurgia International* 14: 45–48.

Ahadi A, Matsushita Y, Sawaguchi T, Sun Q and Tsuchiya K (2017) Origin of zero and negative thermal expansion in severely-deformed superelastic NiTi alloy. *Acta Materialia* 124: 79–92.

Ahadi A and Sun Q (2016) Grain size dependence of fracture toughness and crack-growth resistance of superelastic NiTi. *Scripta Materialia* 113: 171–175.

Akgul O, Tugrul H and Kockar B (2020) Effect of the cooling rate on the thermal and thermomechanical behavior of nitihf high-temperature shape memory alloy. *Journal of Materials Research* 35(12): 1572–1581.

ASTM-E1820 (2016) Standard Test Method for Measurement of Fracture Toughness. Technical report, ASTM International, West Conshohocken, PA.

ASTM-E561 (2020) Standard Test Method for KR Curve Determination. Technical report, ASTM International, West Conshohocken, PA.

Bahrami H, Hoseini S and Voyiadjis G (2019a) Fracture analysis of shape memory alloys in martensite and austenite phase based on the voids behavior. *Mechanics of Materials* 137: 103119.

Bahrami H, Hoseini S and Voyiadjis G (2019b) Fracture investigation of the shape memory alloy using GTN model. *Engineering Fracture Mechanics* 216: 106519.

Banks-Sills L and Volpert Y (1991) Application of the cyclic J-integral to fatigue crack propagation of Al 2024-T351. *Engineering Fracture Mechanics* 40(2): 355–370.

Barrera N, Biscari P and Urbano M (2014) Macroscopic modeling of functional fatigue in shape memory alloys. *European Journal of Mechanics - A/Solids* 45: 101–109.

Baxevanis T and Lagoudas D (2015) Fracture Mechanics of Shape Memory Alloys: Review and Perspectives. *International Journal of Fracture* 191(1-2): 191–213.

Baxevanis T, Parrinello A and Lagoudas D (2016) On the Driving Force for Crack Growth During Thermal Actuation of Shape Memory Alloys. *Journal of the Mechanics and Physics of Solids* 89: 255–271.

Benafan O, Brown J, Calkins F, Kumar P, Stebner A, Turner T, Vaidyanathan R, Webster J and Young M (2014) Shape memory alloy actuator design: CASMART collaborative best practices and case studies. *International Journal of Mechanics and Materials in Design* 10(1): 1–42.

Benafan O and Gaydosh D (2018) Constant-torque thermal cycling and two-way shape memory effect in $Ni_{50.3}Ti_{29.7}Hf_{20}$ torque tubes. *Smart Materials and Structures* 27(7): 075035.

Benafan O, Moholt M, Bass M, Mabe J, Nicholson D and Calkins F (2019) Recent advancements in rotary shape memory alloy actuators for aeronautics. *Shape Memory and Superelasticity* 5(4): 415–428.

Bertacchini O, Lagoudas D and Patoor E (2003) Fatigue life characterization of shape memory alloys undergoing thermomechanical cyclic loading. In: *Smart Structures and Materials 2003: Active Materials: Behavior and Mechanics*, volume 5053. International Society for Optics and Photonics, pp. 612–624.

Bertacchini O, Lagoudas D and Patoor E (2009) Thermomechanical transformation fatigue of TiNiCu SMA actuators under a corrosive environment — Part I: Experimental results. *International Journal of Fatigue* 31(10): 1571–1578.

Bhaumik S, Saikrishna C, Ramaiah K and Venkataswamy M (2008) Understanding the fatigue behaviour of NiTiCu shape memory alloy wire thermal actuators. In: *Key Engineering Materials*, volume 378. Trans Tech Publ, pp. 301–316.

Bigeon M and Morin M (1996) Thermomechanical study of the stress assisted two way memory effect fatigue in TiNi and CuZnAl wires. *Scripta Materialia* 35(12): 1373–1378.

Calhoun C, Wheeler R, Baxevanis T and Lagoudas D (2015) Actuation fatigue life prediction of shape memory alloys under the constant-stress loading condition. *Scripta Materialia* 95: 58–61.

Casati R, Passaretti F and Tuissi A (2011) Effect of electrical heating conditions on functional fatigue of thin NiTi wire for shape memory actuators. *Procedia Engineering* 10: 3423–3428.

Chen J, Yin H and Sun Q (2020) Effects of grain size on fatigue crack growth behaviors of nanocrystalline superelastic NiTi shape memory alloys. *Acta Materialia* 195: 141–150.

Cisse C, Zaki W and Zineb T (2016) A review of modeling techniques for advanced effects in shape memory alloy behavior. *Smart Materials and Structures* 25(10): 103001.

Cocco V, Iacoviello F, Maletta C and Natali S (2014) Cyclic microstructural transitions and fracture micromechanisms in a near equiatomic NiTi alloy. *International Journal of Fatigue* 58: 136–143.

Dlouhý A, Khalil-Allafi J and Eggeler G (2004) On the determination of the volume fraction of Ni_4Ti_3 precipitates in binary Ni-rich NiTi shape memory alloys. *Zeitschrift fur Metallkunde* 95(6): 518–524.

Dunand-Châtellet C and Moumni Z (2012) Experimental analysis of the fatigue of shape memory alloys through power-law statistics. *International Journal of Fatigue* 36(1): 163–170.

Eggeler G, Hornbogen E, Yawny A, Heckmann A and Wagner M (2004) Structural and functional fatigue of NiTi shape memory alloys. *Materials Science and Engineering A* 378: 24–33.

Eleftheroglou N, Zarouchas D and Benedictus R (2020) An adaptive probabilistic data-driven methodology for prognosis of the fatigue life of composite structures. *Composite Structures* 245: 112386.

Fullwood D, Niezgoda S, Adams B and Kalidindi S (2010) Microstructure sensitive design for performance optimization. *Progress in Materials Science* 55(6): 477–562.

Gall K, Yang N, Sehitoglu H and Chumlyakov Y (1998) Fracture of precipitated NiTi shape memory alloys. *International Journal of Fracture* 109: 189–207.

Gehring D, Monroe J and Karaman I (2020) Effects of composition on the mechanical properties and negative thermal expansion in martensitic TiNb alloys. *Scripta Materialia* 178: 351–355.

Gollerthan S, Young M, Baruj A, Frenzel J, Schmahl W and Eggeler G (2009a) Fracture Mechanics and Microstructure in NiTi Shape Memory Alloys. *Acta Materialia* 57(4): 1015–1025.

Gollerthan S, Young M, Neuking K, Ramamurty U and Eggeler G (2009b) Direct Physical Evidence for the Back-Transformation of Stress-Induced Martensite in the Vicinity of Cracks in Pseudoelastic NiTi Shape Memory Alloys. *Acta Materialia* 57(19): 5892–5897.

Haghgouyan B, Hayrettin C, Baxevanis T, Karaman I and Lagoudas D (2019) Fracture toughness of NiTi–Towards establishing standard test methods for phase transforming materials. *Acta Materialia* 162: 226–238.

Haghgouyan B, Young B, Picak S, Baxevanis T, Karaman I and Lagoudas D (2021) A unified description of mechanical and actuation fatigue crack growth in shape memory alloys. *Acta Materialia* 217: 117155.

Hartl D and Lagoudas D (2007) Aerospace applications of shape memory alloys. Proceedings of the Institution of Mechanical Engineers, Part G: Journal of Aerospace Engineering. SAGE, pp. 535–552.

Harvey S, Marsh P and Gerberich W (1994) Atomic force microscopy and modeling of fatigue crack initiation in metals. *Acta Metallurgica et Materialia* 42(10): 3493–3502.

Hasan M and Baxevanis T (2019) Actuation fatigue life prediction of notched shape memory alloy members. *Journal of Applied Mechanics* 86(6): 064501.

Hazeli K, Askari H, Cuadra J, Streller F, Carpick R, Zbib H and Kontsos A (2015) Microstructure-sensitive investigation of magnesium alloy fatigue. *International Journal of Plasticity* 68: 55–76.

Honarmandi P, Hossain M, Arroyave R and Baxevanis T (2021) A Top-Down Characterization of NiTi Single-Crystal Inelastic Properties within Confidence Bounds through Bayesian Inference. *Shape Memory and Superelasticity* 7(1): 50–64.

Hornbogen E (2004) Review: Thermo-mechanical fatigue of shape memory alloys. *Journal of Materials Science* 39(2): 385–399.

Hornbogen E and Eggeler G (2004) Surface aspects in fatigue of shape memory alloys (SMAs). *Materialwissenschaft und Werkstofftechnik: Entwicklung, Fertigung, Prüfung, Eigenschaften und Anwendungen technischer Werkstoffe* 35(5): 255–259.

Icardi U and Ferrero L (2009) Preliminary study of an adaptive wing with shape memory alloy torsion actuators. *Materials & Design* 30(10): 4200–4210.

Iliopoulos A, Steuben J, Kirk T, Baxevanis T, Michopoulos J and Lagoudas D (2017) Thermomechanical Failure Response of Notched NiTi Coupons. *International Journal of Solids and Structures* 125: 265–275.

Jape S, Baxevanis T and Lagoudas D (2016) Stable Crack Growth During Thermal Actuation of Shape Memory Alloys. *Shape Memory and Superelasticity* 2(1): 104–113.

Jape S, Baxevanis T and Lagoudas D (2018) On the Fracture Toughness and Stable Crack Growth in Shape Memory Alloy Actuators in the Presence of Transformation-Induced Plasticity. *International Journal of Fracture* 209(1): 117–130.

Jape S, Young B, Haghgouyan B, Hayrettin C, Baxevanis T, Lagoudas D and Karaman I (2021) Actuation-induced stable crack growth in near-equiatomic nickel-titanium shape memory alloys: Experimental and numerical analysis. *International Journal of Solids and Structures* 221: 165–179.

Jensen D (2005) Biaxial Fatigue Behavior of NiTi Shape Memory Alloy. Technical report, Air Force Institute of Technology, Wright-Patterson Air Force Base, Ohio.

Kang G and Song D (2015) Review on structural fatigue of NiTi shape memory alloys: Pure mechanical and thermo-mechanical ones. *Theoretical and Applied Mechanics Letters* 5(6): 245–254.

Karakoc O, Hayrettin C, Bass M, Wang S, Canadinc D, Mabe J, Lagoudas D and Karaman I (2017) Effects of upper cycle temperature on the actuation fatigue response of nitihf high temperature shape memory alloys. *Acta Materialia* 138: 185–197.

Karakoc O, Hayrettin C, Canadinc D and Karaman I (2018) Role of applied stress level on the actuation fatigue behavior of nitihf high temperature shape memory alloys. *Acta Materialia* 153: 156–168.

Karakoc O, Hayrettin C, Evirgen A, Santamarta R, Canadinc D, Wheeler R, Wang S, Lagoudas D and Karaman I (2019) Role of microstructure on the actuation fatigue performance of Ni-Rich NiTiHf high temperature shape memory alloys. *Acta Materialia* 175: 107–120.

Karaman I, Evirgen A, Hayrettin C, Noebe R and Ma J (2013) Recent developments in high temperature shape memory alloys. In: *24th Advanced Aerospace Materials and Processes (AeroMat) Conference and Exposition*. ASM.

Kaya I, Özdemir Y, Kaya E and Keskin M (2020) The heating–cooling rate effect on thermal properties of high nickel-rich NiTi shape memory alloy. *Journal of Thermal Analysis and Calorimetry* 139(2): 817–822.

König D, Zarnetta R, Savan A, Brunken H and Ludwig A (2011) Phase transformation, structural and functional fatigue properties of TiNiHf shape memory thin films. *Acta Materialia* 59(8): 3267–3275.

Lagoudas D (2008) *Shape Memory Alloys: Modeling and Engineering Applications*. Springer US.

Lagoudas D, Entchev P, Popov P, Patoor E, Brinson L and Gao X (2006) Shape memory alloys. Part II: Modeling of polycrystals. *Mechanics of Materials* 38: 430–462.

Lagoudas D, Miller D, Rong L and Kumar P (2009) Thermomechanical fatigue of shape memory alloys. *Smart Materials and Structures* 18(8): 085021.

Lamba H (1975) The j-integral applied to cyclic loading. *Engineering Fracture Mechanics* 7(4): 693–703.

Lambert Y, Saillard P and Bathias C (1988) Application of the J concept to fatigue crack growth in large-scale yielding. In: *Fracture mechanics: nineteenth symposium*. ASTM International.

Le J, Xu Z and Eliáš J (2018) Internal length scale of weakest-link statistical model for quasi-brittle fracture. *Journal of Engineering Mechanics* 144(4): 04018017.

Lemaitre J (1986) Local approach of fracture. *Engineering Fracture Mechanics* 25(5): 523–537. DOI:https://doi.org/10.1016/0013-7944(86)90021-4.

Lepage W, Ahadi A, Lenthe W, Sun Q, Pollock T, Shaw J and Daly S (2018) Grain size effects on niti shape memory alloy fatigue crack growth. *Journal of Materials Research* 33(2): 91–107.

Lepage W, Shaw J and Daly S (2021) Effects of texture on the functional and structural fatigue of a NiTi shape memory alloy. *International Journal of Solids and Structures* 221: 150–164.

Li X, Tao Z, Wu J and Zhang W (2021) Uncertainty theory based reliability modeling for fatigue. *Engineering Failure Analysis* 119: 104931.

Mabe J, Ruggeri R, Rosenzweig E and Yu C (2004) Nitinol performance characterization and rotary actuator design. In: *Smart Structures and Materials 2004: Industrial and Commercial Applications of Smart Structures Technologies*, volume 5388. International Society for Optics and Photonics, SPIE, pp. 95 – 109.

Mahtabi M, Shamsaei N and Mitchell M (2015) Fatigue of nitinol: The state-of-the-art and ongoing challenges. *Journal of the Mechanical Behavior of Biomedical Materials* 50: 228–254.

Main B, Jones M and Barter S (2021) The practical need for short fatigue crack growth rate models. *International Journal of Fatigue* 142: 105980.

Makkar J and Baxevanis T (2020) Notes on the experimental measurement of fracture toughness of shape memory alloys. *Journal of Intelligent Material Systems and Structures* 31(3): 475–483. DOI:10.1177/1045389X19888730.

Makkar J and Baxevanis T (2021) On the fracture response of shape memory alloys by void growth and coalescence. *Mechanics of Materials* 153: 103682.

Makkar J, Young B, Karaman I and Baxevanis T (2021a) Experimental observations of “reversible” transformation toughening. *Scripta Materialia* 191: 81–85.

Makkar J, Young B, Karaman I and Baxevanis T (2021b) Fracture resistance of shape memory alloys under thermomechanical loading. *Engineering Fracture Mechanics* Accepted.

Maletta C, Sgambitterra E and Niccoli F (2016) Temperature dependent fracture properties of shape memory alloys: Novel findings and a comprehensive model. *Scientific reports* 6(1): 1–16.

Mammano G and Dragoni E (2014a) Effects of loading and constraining conditions on the thermomechanical fatigue life of NiTi shape memory wires. *Journal of Materials Engineering and Performance* 23(7): 2403–2411.

Mammano G and Dragoni E (2014b) Functional fatigue of NiTi shape memory wires under various loading conditions. *International Journal of Fatigue* 69: 71–83.

McDowell D and Dunne F (2010) Microstructure-sensitive computational modeling of fatigue crack formation. *International Journal of Fatigue* 32(9): 1521–1542.

McEvily A and Matsunaga H (2010) On fatigue striations. *Transaction B: Mechanical Engineering* 17: 75–82.

Meier H, Haberland C and Frenzel J (2012) Structural and functional properties of niti shape memory alloys produced by selective laser melting. In: Bartolo P (ed.) *Innovative Developments in Virtual and Physical Prototyping*, Conference on Advanced Research in Virtual and Rapid Prototyping. Taylor & Francis, pp. 291–296.

Mettu S, Shivakumar V, Beek J, Yeh F, Williams L, Forman R, McMahon J and Newman J (1999) NASGRO 3.0 : A software for analyzing aging aircraft. The Second Joint NASA/FAA/DoD Conference on Aging Aircraft. pp. 792–801.

Monroe J, Gehring D, Karaman I, Arroyave R, Brown D and Clausen B (2016) Tailored thermal expansion alloys. *Acta Materialia* 102: 333–341.

Nespoli A, Besseghini S, Pittaccio S, Villa E and Viscuso S (2010) The high potential of shape memory alloys in developing miniature mechanical devices: A review on shape memory alloy mini-actuators. *Sensors and Actuators A:Physical* 158(1): 149–160.

Neuber H (1960) Theory of stress concentration for shear-strained prismatical bodies with arbitrary nonlinear stress-strain law. *Journal of Applied Mechanics, Transactions ASME* 28(4): 544–550.

Olsen J, Zhang Z, Lu H and van der Eijk C (2012) Fracture of notched round-bar NiTi-specimens. *Engineering Fracture Mechanics* 84: 1–14.

Otsuka K and Wayman C (1999) *Shape memory materials*. Cambridge university press.

Paris P (1964) The fracture mechanics approach to fatigue. In: *10th Sagamore Army Material Research Conference*. Syracuse University Press.

Paris P and Erdogan F (1963) A critical analysis of crack propagation laws. *ASME Journal of Basic Engineering* 85(4): 528–533.

Patoor E, Lagoudas D, Entchev P, Brinson L and Gao X (2006) Shape memory alloys, Part I: General properties and modeling of single crystals. *Mechanics of Materials* 38(5–6): 391–429.

Pelton A (2011) Nitinol fatigue: A review of microstructures and mechanisms. *Journal of Materials Engineering and Performance* 20: 613–617.

Pineau A (2006) Development of the local approach to fracture over the past 25 years: theory and applications. *International Journal of Fracture* 138(1-4): 139–166.

Plotino G, Grande N, Cordaro M, Testarelli L and Gambarini G (2009) A review of cyclic fatigue testing of nickel-titanium rotary instruments. *Journal of Endodontics* 35(11): 1469–1476.

Przybyla C, Prasannavenkatesan R, Salajegheh N and McDowell D (2010) Microstructure-sensitive modeling of high cycle fatigue. *International Journal of Fatigue* 32(3): 512 – 525.

Rabold F and Kuna M (2014) Automated Finite Element Simulation of Fatigue Crack Growth in Three-dimensional Structures with the Software System ProCrack. *Procedia Materials Science* 3: 1099–1104.

Rabold F, Kuna M and Leibelt T (2013) Procrack: A software for simulating three-dimensional fatigue crack growth. *Lecture Notes in Applied and Computational Mechanics* 66: 355–374.

Robertson S, Mehta A, Pelton A and Ritchie R (2007) Evolution of crack-tip transformation zones in superelastic Nitinol subjected to in situ fatigue: A fracture mechanics and synchrotron X-ray microdiffraction analysis. *Acta Materialia* 55(18): 6198–6207.

Robertson S, Pelton A and Ritchie R (2012) Mechanical fatigue and fracture of nitinol. *International Materials Reviews* 57(1): 1–37.

Rovinelli A, Sangid M, Proudhon H and Ludwig W (2018) Using machine learning and a data-driven approach to identify the small fatigue crack driving force in polycrystalline materials. *Computational Materials* 4(1): 1–10.

Saikrishna C, Ramaiah K, Bhagyaraj J, Gouthama and Bhaumik S (2013a) Influence of stored elastic strain energy on fatigue behaviour of NiTi shape memory alloy thermal actuator wire. *Materials Science and Engineering A* 587: 65–71.

Saikrishna C, Ramaiah K, Vidyashankar B and Bhaumik S (2013b) Effect of intermittent overload cycles on thermomechanical fatigue life of NiTi shape memory alloy wire. *Metallurgical and Materials Transactions A* 44(1): 5–8.

Sankararaman S, Ling Y and Mahadevan S (2011) Uncertainty quantification and model validation of fatigue crack growth prediction. *Engineering Fracture Mechanics* 78(7): 1487–1504.

Sawaguchi T, Kausträter G, Yawny A, Wagner M and Eggeler G (2003) Crack initiation and propagation in 50.9 At. pct Ni-Ti pseudoelastic shape-memory wires in bending-rotation fatigue. *Metallurgical and Materials Transactions A* 34: 2847–2860.

Schick J (2009) *Transformation induced fatigue of Ni-rich NiTi shape memory alloy actuators*. Master's Thesis, Texas A&M University.

Sgambitterra E, Maletta C, Magarò P, Renzo D, Furgiuele F and Sehitoglu H (2019) Effects of Temperature on Fatigue Crack Propagation in Pseudoelastic NiTi Shape Memory Alloys. *Shape Memory and Superelasticity* 5(3): 278–291.

Shang D, Wang D, Li M and Yao W (2001) Local stress–strain field intensity approach to fatigue life prediction under random cyclic loading. *International Journal of Fatigue* 23(10): 903–910.

Smith K, Watson P and Topper T (1970) Stress–strain function for the fatigue of metals. *Journal of Materials* 5(4): 767–778.

Socie F and Marquis G (1999) *Multiaxial Fatigue*. Society of Automotive Engineers Inc.

Spear A, Kalidindi S, Meredig B, Kontsos A and Graverend J (2018) Data-driven materials investigations: the next frontier in understanding and predicting fatigue behavior. *The Journal of The Minerals, Metals & Materials Society* 70(7): 1143–1146.

Sreekumar M, Nagarajan T, Singaperumal M, Zoppi M and Molfino R (2007) Critical review of current trends in shape memory alloy actuators for intelligent robots. *Industrial Robot* 34(4): 285–294.

Stroud H and Hartl D (2020) Shape memory alloy torsional actuators: a review of applications, experimental investigations, modeling, and design. *Smart Materials and Structures* 29(11): 113001.

Tanaka K (1983) The cyclic j-integral as a criterion for fatigue crack growth. *International Journal of Fracture* 22(2): 91–104.

Tang H, Guo X and Xue S (2020) Uncertainty quantification in small-timescale model-based fatigue crack growth analysis using a stochastic collocation method. *Metals* 10(5): 646.

TerMaath S, Fleishel R, Jordan B, Cauthen C, Daniewicz S and Baker A (2020) Characterization of surface fatigue crack nucleation and microstructurally small crack growth in high strength aluminum alloys. *Frontiers in Materials* 7: 464.

Thumann M and Hornbogen E (1988) Thermal and mechanical fatigue in Cu-based shape memory alloys. *Zeitschrift fuer Metallkunde/Materials Research and Advanced Techniques* 79(2): 119–126.

Weixing Y (1993) Stress field intensity approach for predicting fatigue life. *International Journal of Fatigue* 15(3): 243–246.

Wheeler R, Ottmers C, Hewling B and Lagoudas D (2016) Actuator lifetime predictions for $Ni_{60}Ti_{40}$ shape memory alloy plate actuators. In: *Proceedings of SPIE - The International Society for Optical Engineering*, volume 9800. DOI:10.1117/12.2219514.

Wheeler R, Santa-Cruz J, Hartl D and Lagoudas D (2013) Effect of processing and loading on equiatomic NiTi fatigue life and localized failure mechanisms. In: *Mechanics and Behavior of Active Materials*, Conference on Smart Materials, Adaptive Structures and Intelligent Systems. ASME, pp. 10.1115/SMASIS2013–3163.

Yao W (1996) The prediction of fatigue behaviours by stress field intensity approach. *Acta Mechanica Solida Sinica* 9: 337–349.

Young B, Haghgouyan B, Lagoudas D and Karaman I (2019) Effect of Temperature on the Fracture Toughness of a NiTiHf High Temperature Shape Memory Alloy. *Shape Memory and Superelasticity* 5(4): 362–373.

Zhang Y, Moumni Z, You Y, Zhang W, Zhu J and Anlas G (2019) Multiscale trip-based investigation of low-cycle fatigue of polycrystalline niti shape memory alloys. *International Journal of Plasticity* 115: 307–329.

Zheng L, He Y and Moumni Z (2017) Investigation on fatigue behaviors of NiTi polycrystalline strips under stress-controlled tension via in-situ macro-band observation. *International Journal of Plasticity* 90: 116–145.